Semiconductor Optoelectronics
ISSN: 1001-5868

STRUCTURAL, OPTICAL, ELEMENTAL, MORPHOLOGICAL AND THERMAL CHARACTERISTICS OF PURE AND OXALIC ACID-DOPED GROWTH THIOUREA SINGLE CRYSTALS

D.PriyaDharshini [1], C.Hentry[2], B.Leema Rose [3]

[1]Research Scholar (Reg.no: 19213232132011), Department of Physics, St. Jude's College, Thoothoor, Affiliated to Manonmaniam Sundaranar University, Abishekapatti, Tirunelveli, 627012, Tamilnadu, India

[2] Department of Physics, St. Jude's College, Thoothoor, 629176, Tamilnadu, India

[3] Department of Physics, St. Jude's College, Thoothoor, 629176, Tamilnadu, India

Abstract

The growth of single crystals of pure and Oxalic Acid (OA)-doped Thiourea (TU) was accomplished by solvent evaporation. The grown crystals were characterised by Single crystal X-ray diffraction, X-ray powder diffraction, FTIR, EDAX, SEM, UV-visible, and TG/DTA techniques. The OA-doped TU crystal has good optical transmission in the entire visible range. The UV-visible transmittance shows that the 0.5 M% OA doped TU and 1 M% doped TU at the lower cut-off wavelength was found to be reduced by 139.9 nm and 141.1 nm, compared to pure TU, which is an essential requirement for a nonlinear optical material.

Key words: Optical material, Oxalic Acid, Gravimetric, Structural resemblance, Thiourea

1. Introduction

Low-temperature solution growth is the simplest and, in many cases, the least expensive method for the production of optical crystals. Nonlinear optical materials (NLO) have a number of applications, such as second harmonic generation, frequency mixing, electro optic modulation, etc. Organic NLO materials are attracting investigators for possible use in optical devices because of their large optical nonlinearity, low cut-off wavelength, short response time, and high laser damage threshold [1]. TU is an interesting inorganic matrix modifier, and it has the ability to form an extensive network of hydrogen bonds [2]. TU inorganic metal complex crystals with interesting optical, crystalline perfection, dielectric, mechanical, and electronic properties, as evidenced by investigators, are bis(TU) cadmium chloride, bis(TU) zinc chloride, bis(TU) cadmium acetate, bis(TU) cadmium acetate [3,4], etc. The molecular structure of TU has been investigated using C2 symmetry constraints [5]. TU, also called thiocarbamide, an organic compound that resembles urea. But contains sulphur instead of oxygen, ie, the molecular formula is $CS(NH_2)_2$, while that of urea is $CO(NH_2)_2$. Like urea, it can be prepared by causing a compound to undergo rearrangement, as by heating ammonium thiocyanate(NH_4SCN). A method of preparation more commonly used consists of the addition of hydrogen sulfide to cyanamide. TU exhibits many of the chemical properties of urea, but it has little commercial application. Organic ligands and small-electron systems such as TU, thiocynate, and urea have been used with remarkable success. The Centro symmetric TU molecule, when combined with an inorganic salt, yields non-Centro symmetric complexes,

which have NLO properties [6]. TU crystals also exhibit a pyro electric effect, which is utilised in infrared (IR), ultraviolet (UV), scanning electron microscopy (SEM), and infrared imaging [7]. TU is one of the few simple organic compounds with high crystallographic symmetry. It crystallises in the rhombic pyramidal division of the rhombic system and acts as a good ligand [8]. TU forms a number of NLO-active metal coordination compounds [9-13].

In the present investigation, pure and various mole percentages of OA doped TU have been grown by solvent evaporation technique.

2. Experimental

2.1. Materials

All the reagents used in the present study were of analytical grade. Thiourea (99%) was purchased from Merck. The solvent used in all the experiments was double-distilled water.

2.2. Temperature dependence on solubility

The maximum amount of solute that dissolves in a known quantity of solvent at a certain temperature is its solubility. Temperature will affect solubility. In the present investigation, the solubility of TU and OA-doped TU in double-distilled water was estimated at various temperatures ranging from 25ºC to 50ºC in steps of 5ºC by the gravimetric method and presented in Table 1.

Table 1. Solubility of TU and Oxalic acid-doped TU in double-distilled water

Temperature (ºC)	Solubility pure TU g/L	Solubility OA doped TU
25	141.5	145.5
30	163.9	169.2
35	190.5	196.5
40	234.5	240.4
45	280.2	286.2
50	414.9	421.5

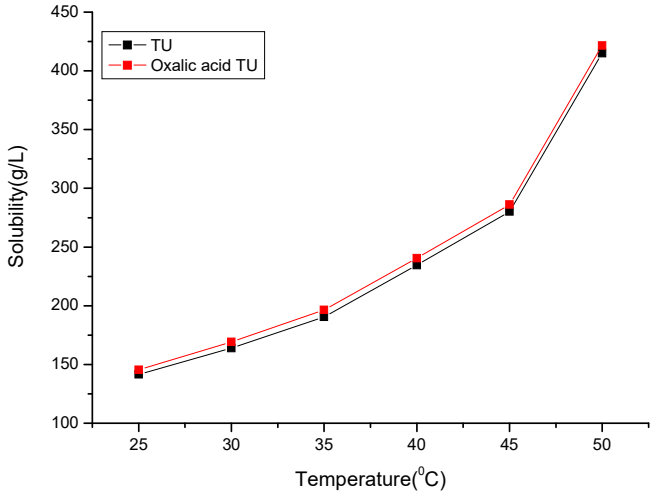

Fig. 2. Solubility curve of TU and OA doped TU

The collected data shows that the solubility of TU increases with an increase in temperature; the addition of OA to the pure TU solution increased the solubility and had a positive temperature coefficient of solubility.

2.3. Crystal growth

150 ml of saturated solution of TU was dissolved in double-distilled water using a magnetic stirrer at a constant rate for 6 hours at a temperature of 30º C. After attaining saturation, the solution was filtered using Whattman filter paper of porous size 11.5mm. A clean and dry 250-ml beaker was used in the present investigation. 50 ml of the saturated solution was taken from three such bakers. One beaker was left as standard for pure TU solution. In all the other beakers, the solution was doped with 0.5 M% and 1 M% of Oxalic acid. All the crystallizers were covered with perforated polythene paper and kept on a vibration-free platform. After a period of 21 days, fully matured pure TU and 56 days, fully matured Oxalic acid_doped TU could be grown. Fig. 3. (a) shows the crystal of pure TU; (b), (c), and (d) show the 0.5 M% of OA doped TU crystals; (e), (f),(g)(h) and (i) show the 1 M% of OA doped TU crystals. The morphology of the TU crystals changed as the concentration of the dopant increased.

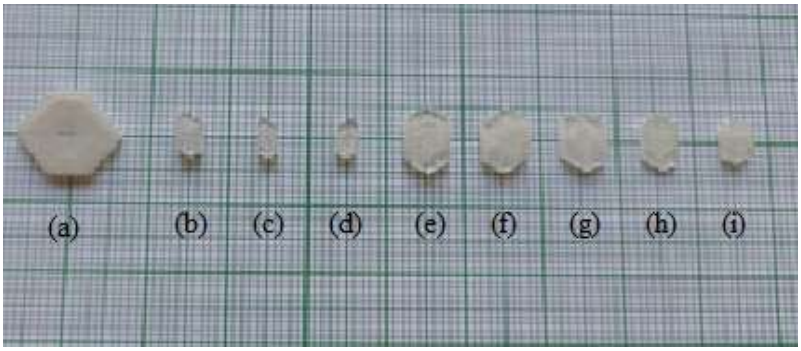

Fig. 3.Crystal habit of (a) TU; (b),(c) and (d) 0.5 M% OA doped TU; (e),(f),(g),(h) and (i) 1 M% OA doped TU

2.4. Characterization

The structural analysis is represented by the details from the Single crystal X-ray diffractometer (Bruker D8 QUEST). Powder X-ray diffractometer (P-Analytical X-Pert-Pro-Diffractometer system with cuKα (Kα=1.54060 ºA) radiation 2θ range at 10˚ - 90˚). The optical studies are performed using Fourier transform infrared spectroscopy (FTIR-Perkin Elmer wavelength range of 4500 cm^{-1} to 500 cm^{-1}). Micro morphological studies of energy dispersive x-ray analysis (EDXA, BRUKER).UV-Visible spectrophotometer (Perkin Elmer Lambda-35 UV-Vis range at 200-800 nm). Thermal analysis studies are carried out using thermal gravimetric and differential thermal analysis (TGA/DTA, NETZSCH STA 2500 at a heating rate of 20°C/min in the temperature range of 30°C to 500°C).

3. RESULTS AND DISCUSSION

3.1. Structural analysis

3.1.1. Single crystal XRD study

The grown crystals were subjected to single-crystal X-ray diffraction analysis using a single-crystal X-ray diffractometer to determine the cell parameters, and it was revealed that the pure

TU, 0.5 M% of OA, and 1 M% of OA doped TU crystals belong to the orthorhombic crystal system with the space group P. The lattice parameters of pure TU were found to be a = 7.6650 Å, b = 8.5539 Å, c = 5.4883 Å, α = 90º, β = 90º, γ = 90º and the cell volume is V = 360 $Å^3$. The lattice parameters of 0.5 M% OA were found to be a = 7.6651 Å, b = 8.5557 Å, c = 5.4902 Å, α = 90º, β = 90º, γ = 90º and the cell volume is V = 360 $Å^3$. The lattice parameters of 1 M% of OA were found to be a = 7.6676 Å, b = 8.5522 Å, c = 5.4891 Å, α = 90º, β = 90º, γ = 90º and the cell volume is V = 360 $Å^3$. The crystallographic data for pure TU, 0.5 M% of OA and 1 M% of OA doped TU crystals are given in table 2. In case of the doped samples, a slight variation in the cell parameters is observed, which may due to the incorporation in thiourea. This analysis revealed that the pure TU, 0.5 M% of OA and 1 M% of OA doped TU crystals does not change the crystal system through there is a small change in the lattice parameters. The structural information for crystals of pure TU, doped with 0.5 M% of OA, and doped with 1 M% of OA is the incorporation of thiourea may be the cause of the minor difference in cell parameters seen in the doped samples. This analysis showed that the crystal system is unaffected by the pure TU, 0.5 M% of OA, and 1 M% of OA doped TU crystals, but the lattice properties are somewhat altered.

Table 2. Single crystal XRD Cell parameters of Pure and OA doped TU

Cell parameters(Aº)	Calculated value of TU (Aº)	0.5 M% OA doped TU(Aº)	1 M% OA doped TU(Aº)
a	7.6650	7.6651	7.6676
b	8.5539	8.5557	8.5522
c	5.4883	5.4902	5.4891
Cell volume (A^3)	360	360	360
Crystal System and space group	Orthorhombic P	Orthorhombic P	Orthorhombic P

3.1.2. Powder XRD Study

The powder XRD patterns of pure TU, 0.5 M% of OA and 1 M% of OA doped TU crystals are shown in fig.4. (a), (b), and (c) respectively.

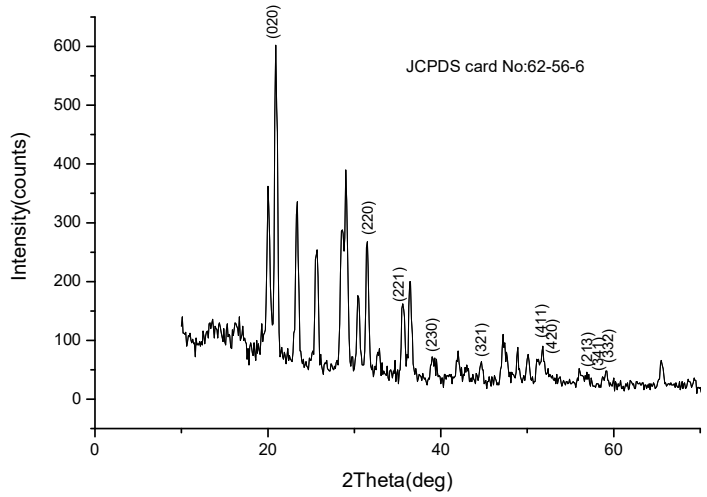

Fig. 4(a) XRD spectrum of pure TU

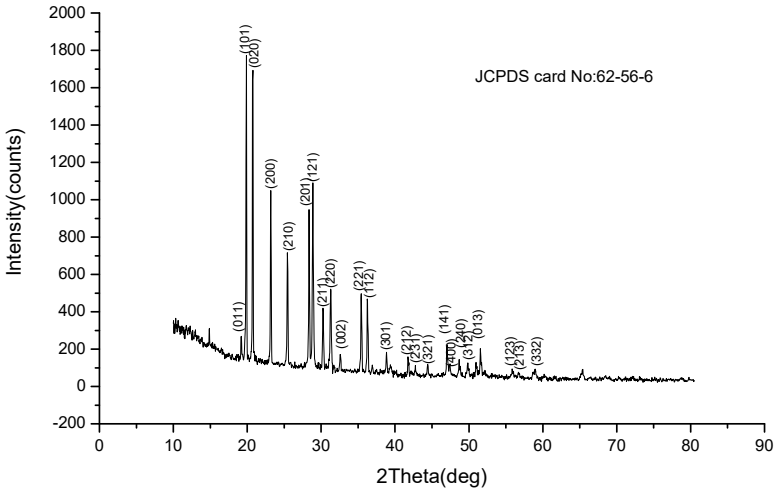

Fig. 4(b) XRD spectrum of 0.5 M% of OA doped TU

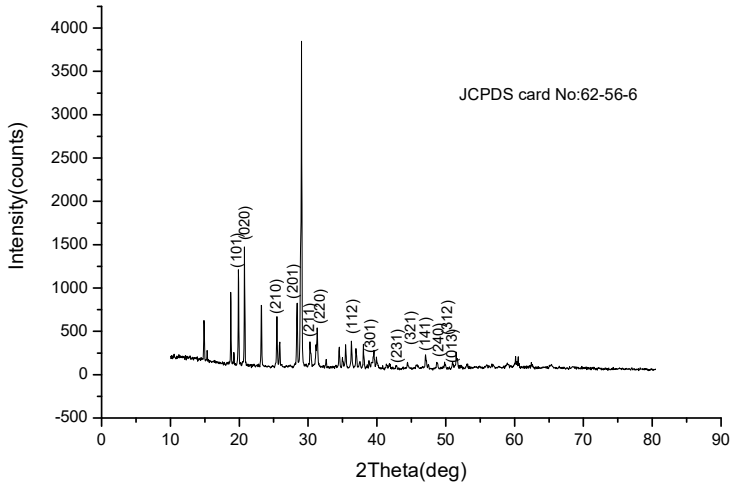

Fig. 4(c) XRD spectrum of 1 M% OA doped TU

Table 3. Powder XRD Cell parameters of Pure and OA doped TU

Cell parameters (Aº)	JCPDS value of TU (Aº)	Reference value of TU (Aº)[14]	Calculated value of TU (Aº)	0.5 M% OA doped TU(Aº)	1 M% OA doped TU(Aº)
A	7.664	7.644	7.646	7.663	7.660
B	8.559	8.527	8.564	8.563	8.552
C	5.492	5.493	5.474	5.491	5.490
Cell volume (A^3)	360.31	358.04	358.45	360.38	359.73

The powder XRD pattern reveals an orthorhombic crystal system. The space group of the pure and OA doped TU crystals was Pnma 62. Fig.4(a) shows the sharp peaks of pure crystal, revealing the crystallinity of grown crystals. The peak observed in the powder XRD pattern was indexed properly. The cell parameters are calculated, and the results of the cell software and the results of the cell parameters were a=7.646˚ A, b=8.564˚A and c=5.474˚ A. The calculated cell volume of the pure crystal is 358.45˚ A^3.

Fig.4(b) shows the sharp peaks of 0.5 M% of OA doped TU crystals that reveal the crystallinity of grown crystals. The cell parameters were calculated for the observed XRD pattern by using unit cell software, and the results of the cell software and the results of the cell parameters was a=7.663˚ A, b=8.563˚ A and c=5.491˚ A. The calculated cell volume of the crystal is 360.38˚ A^3.

Fig.4(c) shows the sharp peaks 1 M% of OA doped TU crystals that reveal the crystallinity of grown crystals. The cell parameters were calculated for the observed XRD pattern by using unit cell software, and the results of the cell software and the results of the cell parameters were a=7.660˚ A, b=8.552˚ A and c=5.490˚ A. The calculated cell volume of the crystal is 359.73˚

A^3.

The observed XRD pattern well matched standard JCPDS card No: 62-56-6 and the reported value, and we found a small change in the unit cell parameters in the OA doped TU crystals. The change in unit cell parameters of the OA doped crystals may be due to the presence of Oxalic ions in the crystal lattice.

3.2. Vibrational Analysis

The FTIR spectra of pure TU, 0.5 M% of OA and 1 M% of OA doped TU are presented in fig. 5. (a), (b), and (c), respectively.

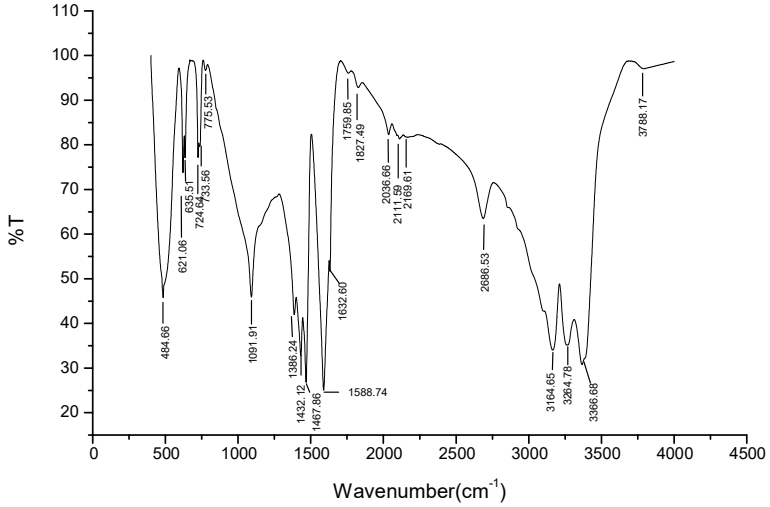

Fig. 5(a) FTIR spectrum of pure TU

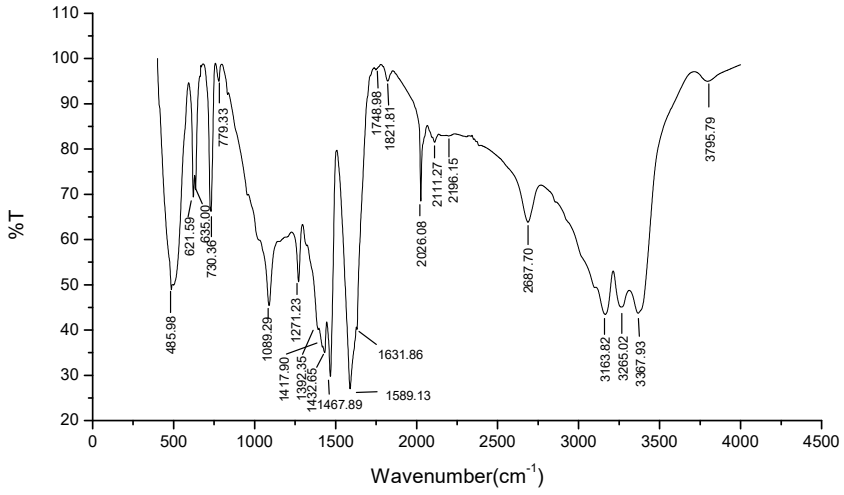

Fig. 5(b) FTIR spectrum of 0.5 M% of OA doped TU

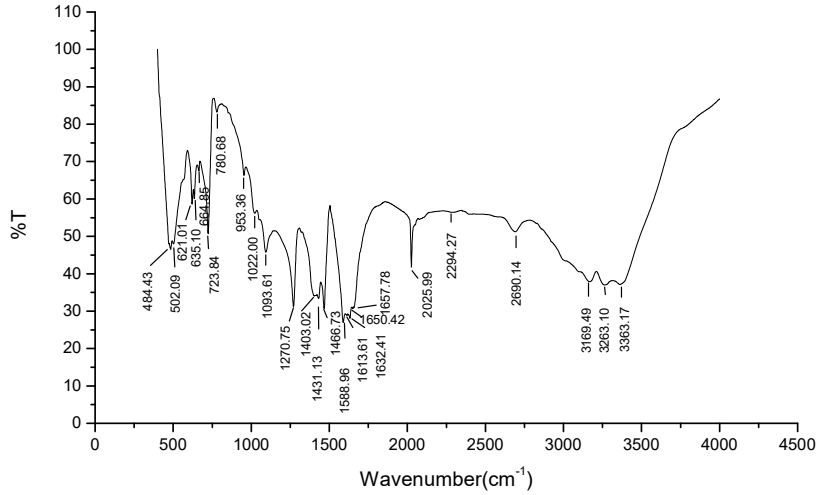

Fig. 5(c) FTIR spectrum of 1 M% of OA doped TU

Table 4.Wave number assignments for pure, 0.5 M% of OA and 1 M% of OA doped TU in cm^{-1}

Pure TU	0.5 M% of OA doped TU	1 M% of OA doped TU	Spectral Assignment
484.66	485.98	484.43	C-N-C Bending
-	-	502.09	C-I Stretch
621.06	621.59	621.01	S-O Stretching
635.51	635.00	635.10	C-H Wag
-	-	664.85	O-H Out-of-plane bend
724.67	-	723.84	In plane N-O bend
733.56 and 775.53	730.36	-	Aromatic out of plane C-H Stretching
-	779.33	780.68	Aromatic NH2 out of plane bend
-	-	953.36	C-C-C Stretch
-	-	1022.00	Si-O-Si Asymmetric Stretch
1091.91	1089.29	1093.61	C-O-C Asymmetric Stretching
-	1271.23	1270.75	C-N Stretching
1386.24	1392.35	-	C=S Asymmetric Stretching
-	-	1403.02	N-O Stretch

-	1417.90	-	Acid in plane O-H Bend
1432.12	1432.65	1431.13	C-N Stretching
1467.86	1467.89	1466.73	C=S Stretching
1588.74	1589.13	1588.96	N-S Scissoring
-	-	1613.61	Aromatic ring modes
1632.60	1631.86	1632.41	N-H Bending
1759.85 and 1827.49	1748.98 and 1821.81	1650.42 and 1657.78	Symmetric C=O Stretching
-	2026.08	2025.99	C-N Stretching
2036.66	-	-	CH_2 rocking
2111.59 and 2169.61	2111.27	-	C≡C Stretching
-	2196.15	-	C≡N Stretch
2300-3500	2300-3500	2294.27 and2300-3500	NH & CH Stretching vibration
3788.17	3795.79	-	O-H and C-H Stretching

The FTIR spectra of the grown pure and OA doped TU crystals are represented in fig.5. (a), (b), and (c). The spectra of the pure TU and OA doped TU are assigned to the C-N-C bending characteristic form present at peak 484.66 cm^{-1}[15],C-I Stretching characteristic form present at peak 502.09 cm^{-1}, S-O stretching characteristic form present at peak 621.06 cm^{-1}, C-H Wag characteristic form present at peak 635.51 cm^{-1},In plane N-O bend characteristic from present at peak 664.85 cm^{-1}, In plane N-O bend characteristic form present at peak 724.67cm^{-1}, , Aromatic out of plane C-H stretching characteristic form is present at peaks of 733.56 cm^{-1} and 775.53 cm^{-1},Aromatic NH2 out of plane bend characteristic form present at peak 779.33 cm^{-1}, C-C-C Stretch characteristic form present at peak 953.36 cm^{-1}, Si-O-Si Asymmetric Stretch characteristic form present at peak 1022.00 cm^{-1}, C-O-C Asymmetric stretching characteristic form present at peak 1091.91 cm^{-1},C-N Stretching characteristic form present at peak 1271.23 cm^{-1}, C=S Asymmetric Stretching characteristics are present at peak 1386.24 cm^{-1}[16].N-O Stretch characteristic form present at peak 1403.02 cm^{-1}, Acid in plane O-H Bend characteristic form present at peak 1417.90 cm^{-1}, C-N stretching characteristic form is present at peak 1432.12 cm^{-1}, C=S Stretching characteristic form is present at peak 1467.86 cm^{-1},N-S scissoring characteristic form is present at peak 1588.74 cm^{-1},Aromatic ring modes characteristic form is present at peak 1613.61 cm^{-1}, N-H Bending characteristic form is present at peak 1632.60 cm^{-1}, Symmetric C=O stretching characteristic form is present at peaks 1759.85 cm^{-1} and 1827.49 cm^{-1}, C≡N Stretch characteristic form present at peak 2026.08 cm^{-1},CH_2 rocking characteristic form is present at peaks 2036 cm^{-1} [17]. C≡C stretching characteristic form is present at peak2111.59cm^{-1}, C≡C stretching characteristic form is present at peaks 2111.59 and 2169.61 cm^{-1}[18] NH and CH stretching characteristic forms are present at peak 2300–3500 cm^{-1} and O-H and C-H stretching characteristic forms are present at peak

3788.17 cm^{-1} [19], some peaks are absent from the OA doped TU and Pure TU grown crystals due to the incorporation of OA doped TU. The FTIR spectral assignments of pure and OA doped TU are shown in table 4.

3.3. EDAX Analysis

The energy dispersive x-ray (EDAX) analysis is used to identify the elements of the grown pure and OA doped TU crystals find the elemental atomic weight percentage of the grown pure and OA doped TU crystals. The element analysis revealed that the elements are carbon, nitrogen, sulphur and oxygen, which confirms that the samples are pure and OA doped TU. On comparing the elemental data of pure grown crystal, oxygen is the only ones we found in the OA doped TU grown crystal. And the element oxygen is present in the OA doped TU grown crystals. The oxygen element's atomic weight and weight percentages are lower in 0.5 M% of OA doped TU than 1 M% of OA doped TU. The elements of carbon and nitrogen have decreased atomic weights and weight percentages in the OA doped TU. And atomic weight percentages and weight percentages are increased in the 1 M% of OA doped TU crystals. The elemental sulphur atomic weight and weight percentages are increased in the 0.5 M% of OA doped TU. And atomic weights and weight percentages are decreased in the 1 M% of OA doped TU crystals. This may be attributed to the incorporation of OA doped TU. Normally, this analysis does not acknowledge the hydrogen element. So that was the reason pure and OA doped TU and its metal complex element of hydrogen are not presented in the EDAX data of pure and OA doped TU and crystal in Table 4.and Fig. 6.(a), (b), and (c) also

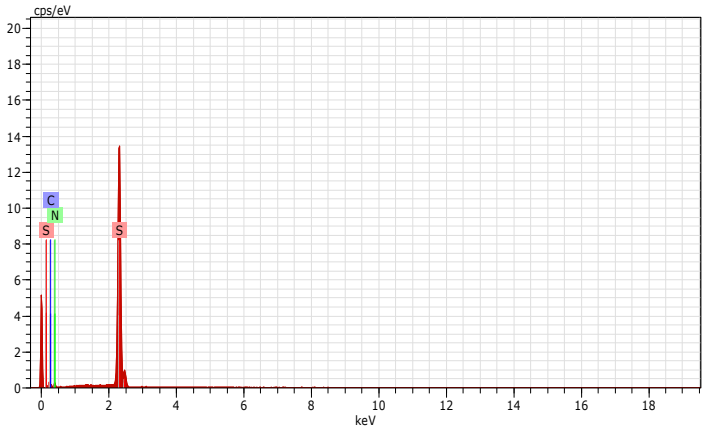

Fig. 6.(a) EDAX spectrum of pure TU crystal

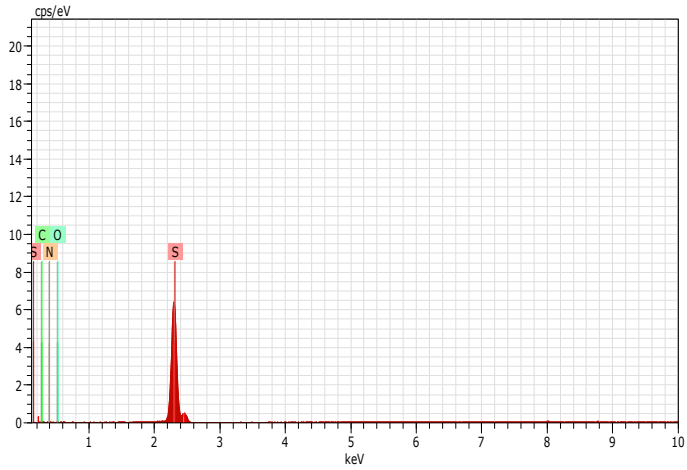

Fig. 6(b) EDAX spectrum of 0.5 M% of OA doped TU crystals

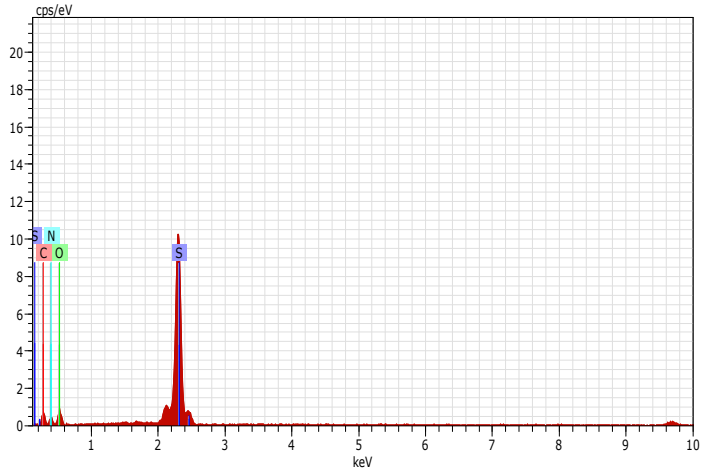

Fig. 6(c) EDAX spectrum of 1 M% of OA doped TU crystals

Table 5. EDAX data of pure and OA doped TU and its metal complexes

Elements	Pure TU		0.5 M% of doped TU		1 M% of OA doped TU	
	At.Wt. %	Weight %	At.Wt. %	Weight %	At.Wt. %	Weight %
C	31.21	18.89	28.16	16.79	36.40	28.15
N	33.02	23.31	27.92	19.42	27.25	24.57
S	35.77	57.80	36.22	57.67	9.52	19.64
0	-	-	7.70	6.12	26.83	27.64

Table 5.shows that in pure TU crystals, only the present elements, such as carbon, nitrogen, and sulphur, were found. But in the OA doped TU, in addition to the parent element, the oxygen element was highly incorporated in the parent element.

3.4. Surface Analysis

The scanning electron microscope (SEM) provides high resolution imaging useful for

evaluating various materials for the crystal surface feature, flaws, contaminants or corrosion. The scanning electron microscope image was used to find surface features of the grown pure TU and 0.5 M% of OA doped TU and 1 M% of OA doped TU crystal from the fig. 7(a),(b) and (c). On visualizing the image of micro morphological grown pure TU and 0.5 M% of OAT doped TU and 1 M% of OA doped TU crystal features of the surface crystal circumstances are found to be smooth showing up the clusters of micro crystalitties were regular and irregular patterns and the crystal structure is orthorhombic.

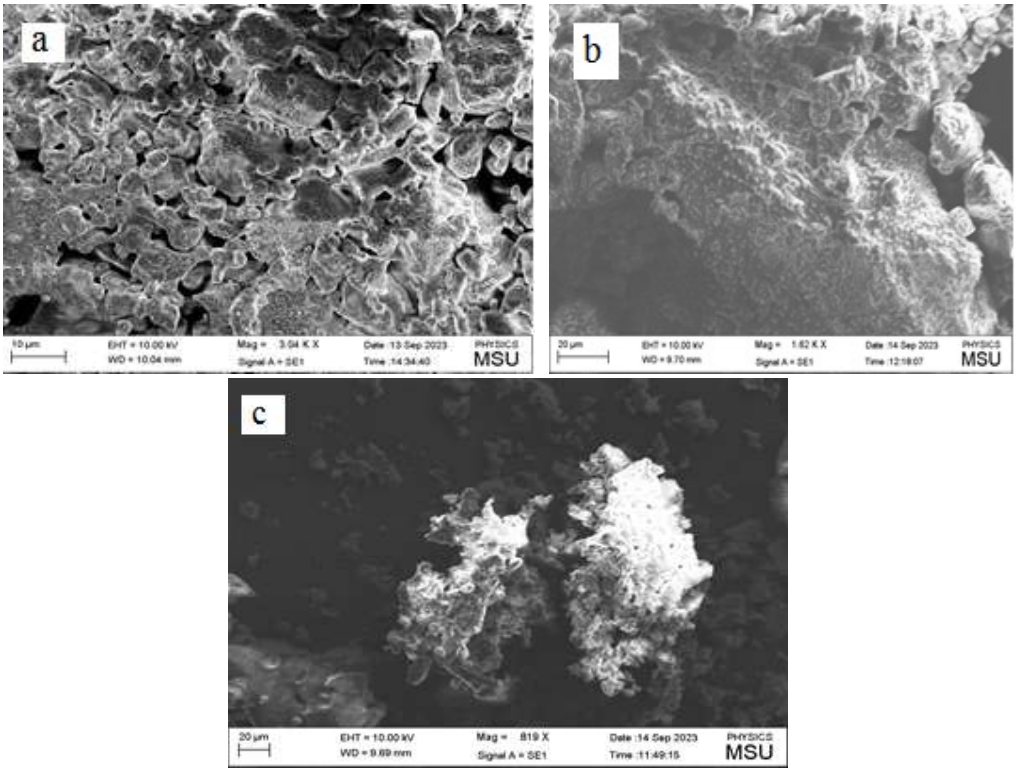

Fig.7 (b). SEM image of grown crystals (a) pure TU ; (b) 0.5 M% of OA doped TU ; (c) 1M% of OA doped TU

3.5. Optical studies

An optical transmission spectrum was recorded using pure and OA doped TU crystal range of 200 to 1200 nm using a Perkin Elmer Lambda 35 UV-Visible spectrometer to know the stability for optical applications. From the spectra in Fig. 8. (a), (b), and (c). It was observed that the pure and OA doped TU crystals showed good transmittance in the entire visible region. The UV cut-off wavelength of pure TU crystal is found to be 376.45 nm, and there is no considerable transmission until 1200 nm. The 0.5 M% of OA doped TU crystals are found to be 236.55 nm and the 1 M% of OA doped TU crystal found to be 235.35 nm; both are slightly decreased, and there is no considerable transmission till 1200 nm [20]. The overlay UV-Vis spectra clearly show the optical quality of grown, pure, and OA doped TU.

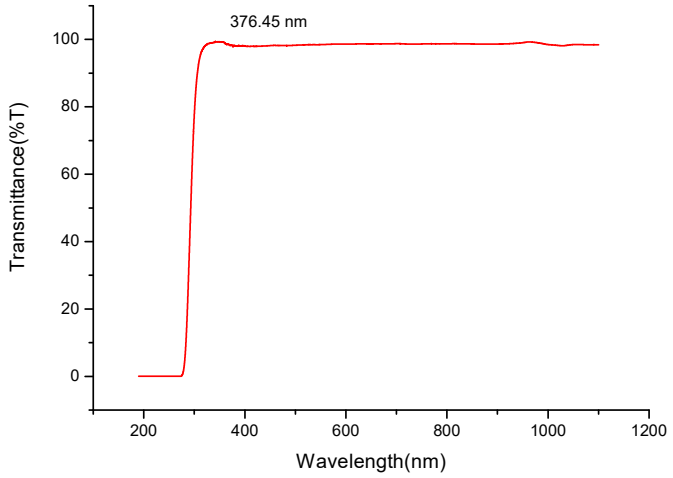

Fig. 8.(a) UV transmittance spectrum of pure TU crystal

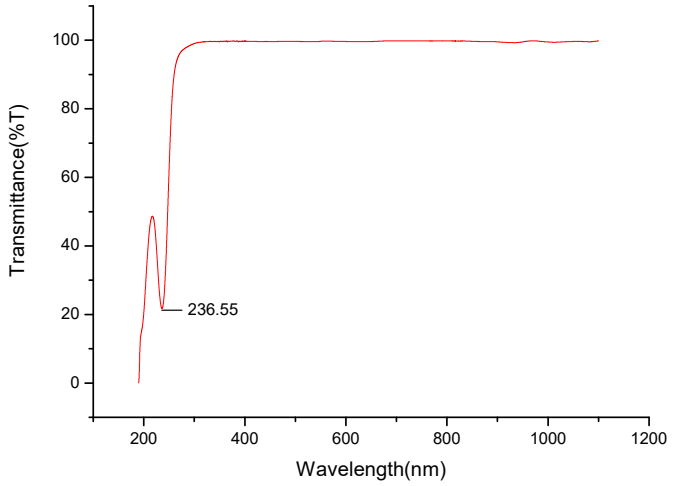

Fig. 8. (b) UV transmittance spectrum of 0.5 M% of OA doped TU crystals

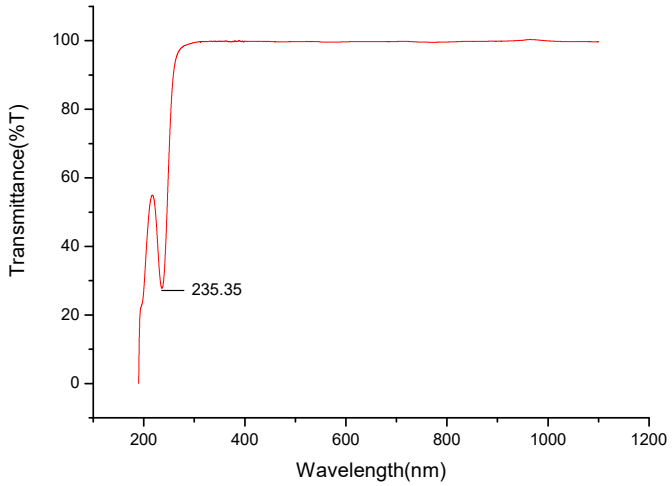

Fig. 8.(c) UV transmittance spectrum of 1 M% of OA doped TU crystals.

According to an optical analysis, the lower cut-off wavelength for pure TU crystals is 376.45 nm. However, it was discovered that the lower cut-off wavelength of the TU crystal with 0.5 M% OA doping was reduced by 139.9 nm, making it 139.9 nm shorter than the pure TU. In comparison to pure TU, the lower cut-off wavelength of the 1 M% OA doped TU crystal was observed to be reduced by 141.1 nm.

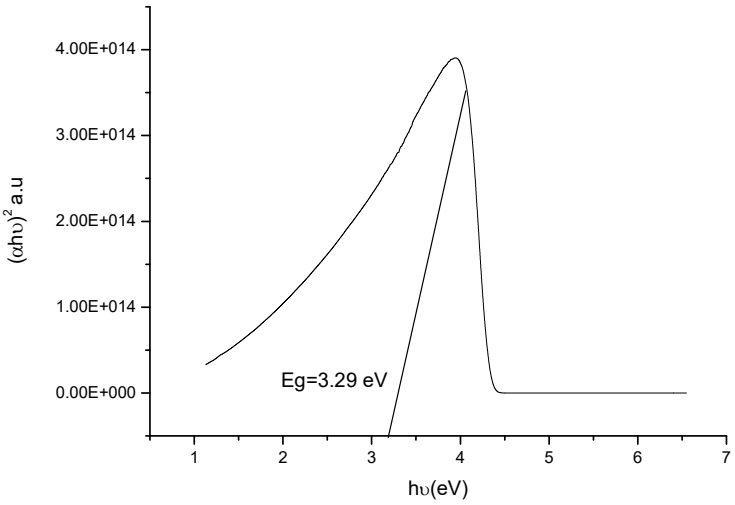

Fig.9 (a) Plot of hν versus $(\alpha h\nu)^2$ of pure TU

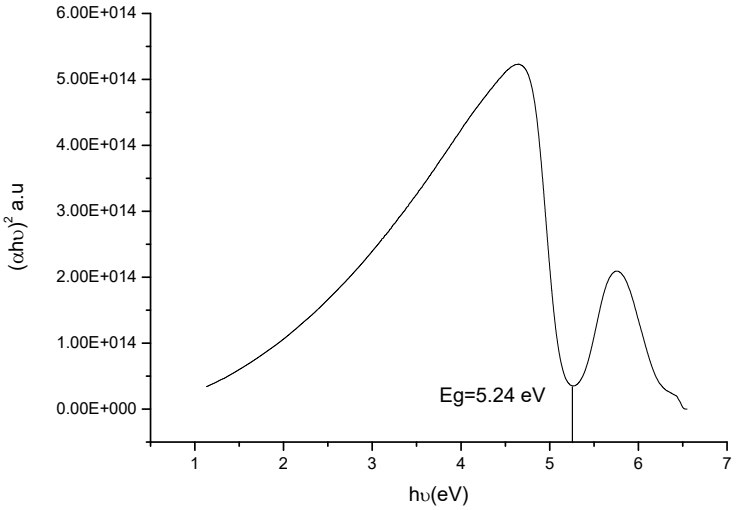

Fig.9 (b) Plot of hν versus $(\alpha h\nu)^2$ of 0.5 M% of OA doped TU

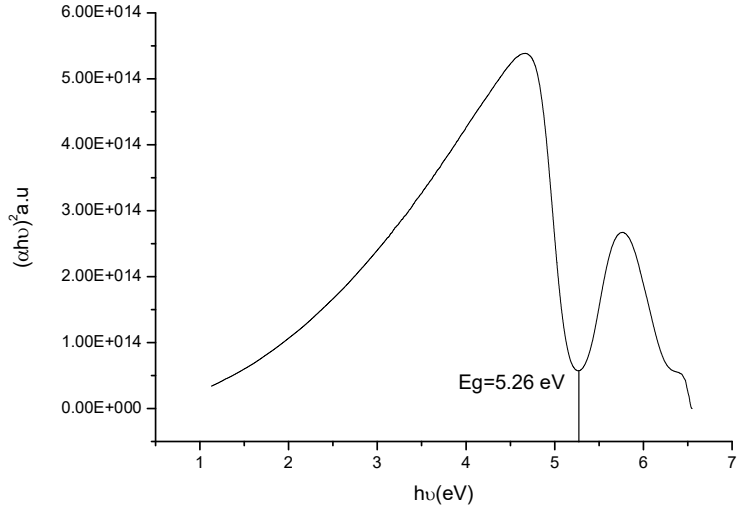

Fig.9 (c) Plot of hν versus $(\alpha h\nu)^2$ of 1 M% of OA doped TU

The plot of hν versus $(\alpha h\nu)^2$ is shown in Fig. 9. (a), (b), and (c) the band gap of pure and OA doped TU. The band gap of pure TU was found to be 3.29 eV, 0.5 M% OA doped TU was found to be 5.24 eV, and 1 M% OA doped TU was found to be 5.26 eV. In this case, the doped samples are increased from the pure TU.

3.6. Thermal Analysis

Thermo gravimetric analysis (TGA) determines decomposition and mass loss over a temperature range. Differential thermal analysis (DTA) determines endothermic and exothermic event temperatures and shows phase transitions. The TGA/DTA analysis was done by delicately grinding the TU, 0.5 M% of OA doped TU and1 M% OA doped TU powdered sample to 0.992 mg placed by the crucible deep A1203 pan for STA2500 to find the thermal

stability of the grown crystals of TU,0.5 M% of OA doped TU and1 M% OA doped TU from thermal analysis by NETZSCH STA 2500 at a heating rate of 20°C/min in the temperature range of 30°C to 500°C under the nitrogen atmosphere. The TGA curve observed by the grown TU crystal is shown in Fig.10(a) shows the decomposition/mass change over a temperature range of up to 30°C and the mass change of -0.91%. The TGA has observed three stages of decomposition and mass change. The first stage of the decomposition of the temperature was noticed at 30°C to 100°C, and the mass change was -0.91%. The second stage was observed at 30°C to 500°C, with a mass change of -93.76%, and the final stage was observed at 100°C to 500°C, with a mass change of -92.88%. The DTA curve shows that in Fig.10(a). It is observed that three fine endothermic peaks are obtained in the grown TU crystal. The starting stage of the endothermic peaks is observed at 180.94°C. The second stage of the endothermic peak of TU observed at 208.44°C. The finishing stage of the endothermic peak of TU was noticed at 458.44°C. This DTA curve shows the TU crystal nature was good, as also determined by the sharpness of the endothermic peaks.

The TGA curve was observed by the grown 0.5 M% of OA doped crystal, as shown in fig. 10(b), which shows the decomposition and mass change over a temperature range up to 30°C and the mass change of -2.66%. The TGA has observed three stages of decomposition and mass change. The first stage of the decomposition of the temperature was noticed at 30°C to 100°C, and the mass change was -2.66%. The second stage was observed at 30°C to 495°C and the mass change was -90.54%, and the final stage was observed at 100°C to 495°C and the mass change was -89.88%. The DTA curve shows that in fig.10(b). It is observed that three fine endothermic peaks are obtained in the grown 0.5 M% OA doped TU crystal. The starting stage of the endothermic peaks is observed at 177.66°C. The second stage of the endothermic peak of 0.5 M% OA doped TU observed at 200.16°C. The finishing stage of the endothermic peak of 0.5 M% OA doped TU was noticed at 462.66°C. This DTA curve shows that the 0.5 M% OA doped TU crystal nature was good, as also determined by the sharpness of the endothermic peaks.

The TGA curve was observed by the grown 1 M% of OA doped crystal, as shown in fig. 10(c), which shows the decomposition and mass change over a temperature range up to 30°C and the mass change of -14.73%. The TGA has observed three stages of decomposition and mass change. The first stage of the decomposition of the temperature was noticed at 30°C to 100°C, and the mass change was -14.73%. The second stage was observed at 30°C to 405°C and the mass change was -100.97%, and the final stage was observed at 100°C to 405°C and the mass change was -98.84%. The DTA curve shows that in fig. 10. (c). It is observed that three fine endothermic peaks are obtained in the grown 1 M% of OA doped TU crystal. The starting stage of the endothermic peaks is observed at 65°C. The second stage of the endothermic peak of 1 M% of OA doped TU observed at 115°C. The finishing stage of the endothermic peak of 1 M% of OA doped TU was noticed at 197.5°C. This DTA curve shows that the 1 M% of OA doped TU crystal nature was good, as also determined by the sharpness of the endothermic peaks.

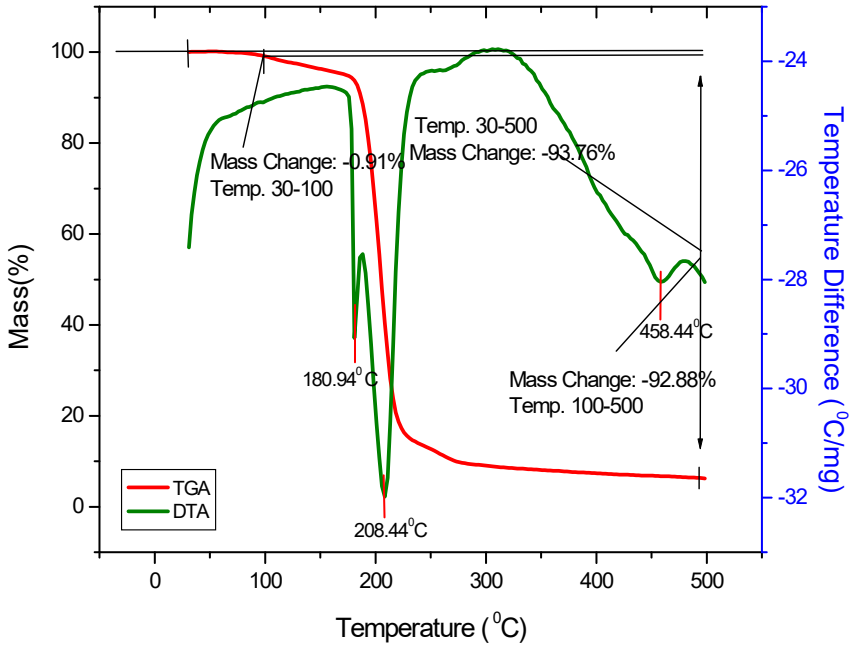

Fig. 10(a) The TGA/DTA curve of the grown TU crystal

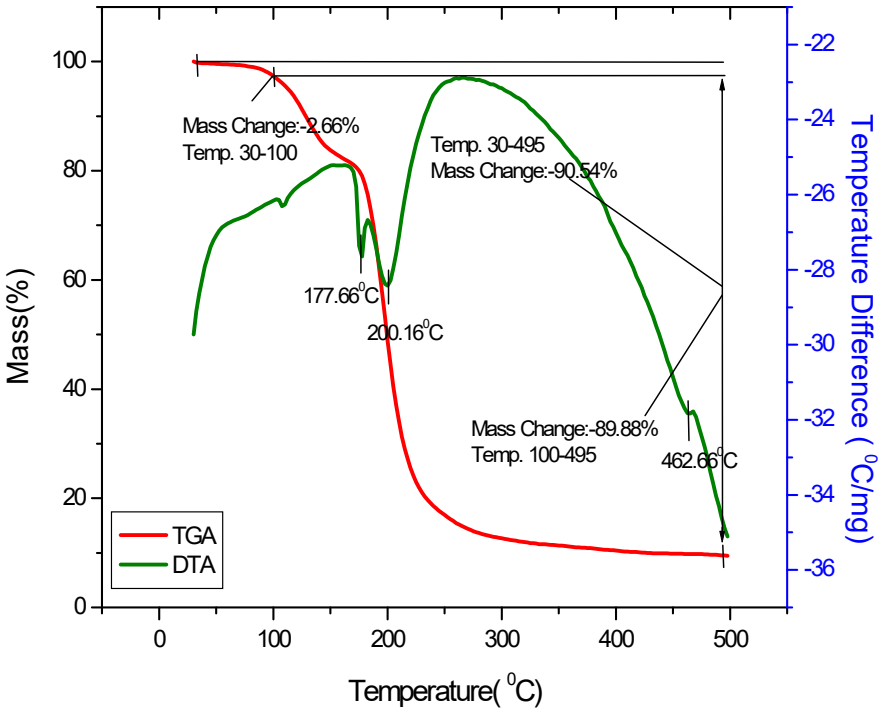

Fig. 10(b) The TGA/DTA curve of the grown 0.5 M% OA doped TU

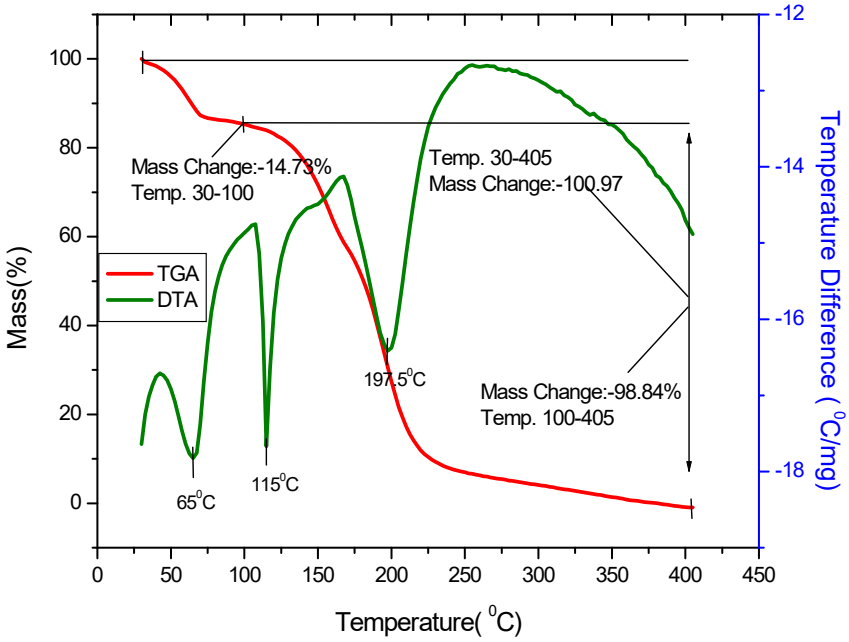

Fig. 10(c) The TGA/DTA curve of the grown 1 M% OA doped TU

Conclusion

Pure and OA doped TU could be grown in various dimensions. The change in the morphology of TU was noticed. The single crystal XRD study indicates that the grown crystals belong to an orthorhombic system with the space group P. The crystallographic data shows a slight variation from TU in the lattice parameters and volume for the doped crystal. The powder XRD study shows that the unit cell volume of the OA doped crystal was slightly decreased and increased from the TU. The FTIR spectrum of pure, OA doped TU shows the incorporation of the dopants. The EDXA analysis confirms the elements present in pure and OA doped TU. The UV-visible transmittance shows that the 0.5 M% OA doped TU and the 1 M% doped TU at the lower cut-off wavelength were found to be reduced by 139.9 nm and 141.1 nm, respectively. The thermal study shows that the metal complex of TU possesses good thermal stability.

References

[1] M. Narayan Bhat, and S.M. Dharma Prakash, Growth of nonlinear optical γ-glycine crystals,Journal of Crystal Growth, 236 (2002) 376-380.https://doi.org/10.1016/S0022-0248(01)02094-2

[2] G.M.S. El-Bahy,B.A. El-Sayed andA.A Shabana,Vibrational and electronic studies on some metal thiourea complexes, Vib. Spectrosc., 31 (2003) 101–107https://doi.org/10.1016/S0924-2031(02)00099-1

[3] R.G. Kumari, V. Ramakrishnan, M.L. Carolin, J. Kumar, A. Sarua, and M. Kuball,Raman spectral investigation of thiourea complexes,SpectrochimicaActa Part A: Molecular and Bimolecular Spectroscopy, 73(2) (2009)263–267.https://doi.org/10.1016/j.saa.2009.02.009

[4] Michel Fleck and Aram M. Petrosyan,Difficulties in the growth and characterization of non-linear optical materials: A case study of salts of amino acids, J.Cryst.Growth, 312 (2010) 2284-2290.https://doi.org/10.1016/j.jcrysgro.2010.04.054

[5] Cristina Puzzarini., Molecular Structure of Thiourea,University of Bologna The journal of physical chemistry A, 116(17) (2012) 4381. https://doi.org/10.1021/jp301493b
[6] A. Anie Roshan, Cyriac Joseph., M.A. Ittyachen,Growth and characterization of a new metal-organic crystal: potassium thiourea bromide, Mater Lett.,49 (2001) 299.https://doi.org/10.1016/S0167-577X(00)00388-8
[7] K. Sanwal, Pro.Crystal Growth, 19 (1989) 189.
[8] S.B. Hendricks, The crystal structure of urea and the molecular symmetry of thiourea, J.Am.Chem.Soc., 50 (1928) 2455.https://doi.org/10.1021/ja01396a019
[9] S. Selvakumar,J. Packiam Julius,S.A. Rajasekar,A. Ramanand andP. Sagayaraj, Thermal, dielectric and photoconductivity studies on pure, Mg^{2+} and Zn^{2+} doped BTCC single crystals,Mater.Chem.Phys., 93 (2005) 356.https://doi.org/10.1016/j.matchemphys.2005.03.016
[10] S. Selvakumar, K. Rajarajan,S.M. Ravikumar,I. VethaPotheher,D. PremAnand, andP. Sagayaraj, Growth and characterization of pure and metal doped bis(thiourea) zinc chloride single crystals, Cryst.Res.Technol, 41 (2006) 766.https://doi.org/10.1002/crat.200510665
[11] N.P. Rajesh, V. Kannan, M. Ashok,K. Sivaji, P. Santhana Raaghavan, and P. Ramasamy,A new nonlinear optical semi-organic material: cadmium thiourea acetate, J.Cryst.Growth, 262 (2004) 561.https://doi.org/10.1016/j.jcrysgro.2003.10.064
[12] V. Venkataraman, G. Dhanaraj, V.K. Wadhawan, J.N. Sherwood and H.L. Bhat, Crystal growth and defects characterization of zinc tris (thiourea) sulfate: a novel metalorganic nonlinear optical crystal,J.Cryst.Growth.154 (1995) 92. https://doi.org/10.1016/0022-0248(95)00212-X
[13] K. Ambujam, P.C. Thomas, S. Aruna,D. Prem Anand and P. Sagayaraj, Growth and characterization of dichloro tetrakis thiourea nickel single crystals,Cryst.Res.Technol, 41 (2006) 1082.https://doi.org/10.1002/crat.200610726
[14] S. Sivasankaran, S. Illangovan, and S. Arivoli, Synthesis and Characterization of Cerium Urea Thiourea Chloride Single Crystal Developed By Slow Evaporation Method, International Journal of Engineering Science Invention, 6 (10) (2017) 05-11http://www.ijesi.org/papers/Vol(6)10/Version-4/B0610040511.pdf
[15] B. Kannan, P.R. Seshadri, K. Illangovan, and P. Murugakoothan, Growth and Characterisation of Lanthanum Doped Sulphamic Acid Single Crystal, Indian journal of science and Technology, 6(7) (2013) 4909-4911.
[16] G. Santhi, and M. Alagar,Growth and Characterization of Single Crystals of Thiourea and Tartaric Acid Based Compounds, Imperial Journal of Interdisciplinary research (IJIR), 2(1) (2016) 537-541.https://www.researchgate.net/publication/321905814_Growth_and_Characterization_of_Single_Crystals_of_Thiourea_and_Tartaric_Acid_Based_Compounds
[17] R. Kalaivani, A. Darlin Mary, S. Minisha, and J. Johnson, Growth and characterization of pure and glycine doped tris thiourea nickel sulphate (TTNS) single crystals, International Journal of Research and Analytical Reviews(IJRAR), 7(1) (2020) 997-1002.https://www.ijrar.org/papers/IJRAR2001273.pdf
[18] P.N. Jegan Mohan Dass, M. Umarani, Victor Antony Raj and J. Madhavan, Growth and characterization of pure and doped urea L-malic acid, Der PharmaChemica., 5(4) (2013) 262-268.https://www.researchgate.net/publication/288311544_Growth_and_characterization_of_

pure_and_doped_urea_L-malic_acid
[19] Smith, Brain C., Infrared Spectral Interpretation: a systematic approach/ Brain C, Smith. CRC Press LLC, Boca Raton London New York Washington.D.C; (1998)1-265.

[20] Z.P. Zheng and W.H. Fan,First principles investigation of L-alanine in terahertz region,

Journal of biological physics, 38(3) (2012) 405-413.https://doi.org/10.1007%2Fs10867-012-9261-0